



OPEN

CT-radiomics combined with inflammatory indicators for prediction of progression free survival of resectable esophageal squamous cell carcinoma

Yating Wang, Genji Bai, Min Huang & Wei Chen✉

To develop a nomogram model which combined clinical inflammatory indicators and CT radiomics features to predict progression free survival (PFS) in esophageal squamous cell carcinoma (ESCC) after radical operation. 258 ESCC patients receiving surgical operation treatment were retrospectively collected from July 2017 to March 2019. Clinical data, laboratory results, pathology results, pre-operative CT data, and survival outcomes were analyzed. Using cox proportional hazards regression model to assess the relationship between relevant clinicopathological factors and PFS. C-index and calibration curve were used to evaluate the nomogram model. Survival curves were obtained using the Kaplan-Meier and comparisons were made by using the log-rank test. The inflammatory model, radiomics model and nomogram model all have good predictive efficacy for predicting PFS of ESCC patients in both training and test set. Significant differences were found between the nomogram model and inflammatory model and the radiomics model (DeLong test, $Z = 3.869$ and 3.195 , $P < 0.001$, $P = 0.001$). Decision curve analysis (DCA) results revealed the net benefit of nomogram model was better than that of inflammatory model and radiomics model. Kaplan-Meier results showed significant difference in PFS between high-risk and low-risk group in Radscore and nomogram model ($P < 0.001$), and the high-risk group was prone to postoperative recurrence and poor PFS. The nomogram model developed by combining inflammatory indicators and radiomics features, which is helpful for risk stratification and follow-up work, and improving ESCC patients' prognosis.

Keywords Esophageal squamous cell carcinoma, Inflammatory indicators, Radiomics, Nomogram

Esophageal squamous cell carcinoma (ESCC) was prone to early lymph node metastasis and with a poor prognosis¹. According to the latest expert consensus, surgery is still the main treatment of resectable esophageal cancer in order to achieve radical goals, especially for the early and middle stage esophageal cancer patients². Postoperative recurrence and metastasis are the main reason of poor prognosis of esophageal carcinoma. How to use effective methods to predict and improve progression-free-survival (PFS) and overall survival (OS) has become an urgent concern for doctors and patients. Pathological stage, lymph node metastasis, peripheral nerve/vascular invasion and other tumor features are widely considered to be the main prognostic factors of esophageal cancer after radical resection^{3–6}. However, tumor node metastasis (TNM) staging system based on single dimension cannot measure the comprehensive effect of multiple factors in the meantime, and then cannot satisfy the personalized prognosis evaluation. In recent years, many studies showed that the interaction between tumors strongly affects the prognosis of cancer patients. Systemic inflammation is the most representative inter-tumor interaction in tumor patients, which has been shown that it plays a major role in tumor initiation, progression, metastasis and treatment resistance. High inflammatory burden in tumor patients may be associated with poor prognosis^{7–9}. Inflammatory indicators such as neutrophil-lymphocyte ratio (NLR) and platelet-lymphocyte ratio (PLR) reflect immune inflammation, which have been reported in prognosis prediction of esophageal cancer¹⁰. Systemic immune inflammation index (SII) reflects the relationship between tumor-induced inflammation and anti-tumor immune response through the combined effect of neutrophils, platelets, and lymphocytes, which has also been proved to be valuable in predicting the prognosis of solid tumors¹¹.

Department of Medical Imaging, The Affiliated Huaian No.1 People's Hospital of Nanjing Medical University, Huai'an, Jiangsu, China. ✉email: wchen74@163.com

Radiomics is a field of medical imaging analysis that extracts numerous quantitative data from both morphological and functional images, and then selecting and analyzing the most relevant features to correlate with clinical outcomes such as treatment response and survival rates. This approach provides a valuable tool for clinical diagnosis and treatment¹². Previous radiomics studies have shown that objective and quantitative radiomics features may be used as prognostic imaging biomarkers¹³. Radiomics have been applied to many aspects of clinical evaluation of cancers, such as diagnosis, prediction of efficacy, and prognosis^{14–16}. These studies demonstrated the feasibility of using radiomics to construct a nomogram to predict the prognosis of patients with esophageal carcinoma. CT plays major clinical value in preoperative staging, assessment of resectability and curative effect monitoring of esophageal carcinoma. Previous studies have demonstrated the potential prognostic value of CT radiomics features. Yang et al.¹⁷ constructed a nomogram model which can effectively predict whether ESCC patients would achieve pathological complete response (pCR) after neoadjuvant immunochemotherapy(nICT) by integrating CT radiomics with hematological factors and clinicopathological characteristics prior to treatment, contributing to clinical decision-making. The area under curve (AUC) values of the radiomics signature and hematology model reached 0.874 (95% CI: 0.819–0.928) and 0.772 (95% CI: 0.699–0.845), respectively, while the AUC the combined nomogram model reached 0.934 (95% CI: 0.896–0.972), demonstrating its good predictive ability. There have been some studies find a nomogram which combined radiomics features and clinical risk factors can be used to predict the presence of lymph node metastasis among patients with ESCC^{18,19}, while there is no study using a radiomics-clinical nomogram to predict 5-year PFS of ESCC. The objective of this study was to develop an individualized nomogram model which combined clinical inflammatory indicators and CT radiomics features to predict PFS for 5 years after radical ESCC surgery and identify patients with possible poor prognosis at an early stage.

Martials and methods

Data collection

This retrospective study was approved by the Ethics Committee of Affiliated Huaian No.1 People's Hospital of Nanjing Medical University (KY-2022-045-01), and written informed consent was waived by the institutional review board. We retrospectively collected 258 ESCC patients with radical esophagectomy in our hospital between July 2017 and March 2019. Patients were randomly divided into training ($n=180$) and test set ($n=78$) at a ratio of 7:3. To address potential class imbalance issues in our dataset, we performed a sensitivity analysis using random under sampling of the major class. The details of this analysis are provided in Supplementary File. Baseline characteristics were obtained including clinical materials, demographic data, lab findings, pre-operative CT data, pathology findings, and survival results. Inclusion criteria: (1) ESCC was proved by postoperative pathology; (2) Enhanced CT scan was conducted 2 weeks before operation; (3) Intact clinical, pathological and imaging information; (4) Intact follow-up information. Exclusion criteria: (1) Preoperative radiotherapy, chemotherapy or other adjuvant therapy was performed; (2) Too small lesion which was difficult to identify by CT; (3) With other malignancies; (4) Multiple esophageal lesions or the lesion was located at the esophagogastric junction.

Clinical inflammatory indicators and pathological data

Clinical baseline data included gender, age, tumor location, pathological differentiation, pTNM stage, and immunohistochemical results. We retrospectively collected complete blood count (CBC) from patient records before operation. All CBC and classifications were acquired one week prior to surgery. Absolute counting of lymphocytes, monocytes, and platelets were acquired from the CBC information. LMR=lymphocyte-to-monocyte ratio (lymphocyte count/monocyte count); NLR = neutrophil-to-lymphocyte ratio (neutrophil count/lymphocyte count); PLR=platelet to-lymphocyte ratio (platelet count/lymphocyte count); SII = Systemic immune inflammation index (platelet count \times neutrophil count/lymphocyte count).

Follow-up of cases

Regular postoperative follow-up of all patients was initiated through phone, electronic patient records, and certification of death. The follow-up including esophagography, contrast-enhanced CT, endoscopic examination, blood routine and biochemical tests. When suspected of recurrence or metastasis, corresponding imaging examination were performed according to the patient's condition, and comparison is made with the data before surgery. The collected information includes recurrence time and the location of recurrence. Recurrence was mainly according to imaging examination report or pathology results. Local regional recurrence refers to lymph node metastasis in the neck, mediastinum, or upper abdomen, recurrence of tumor bed region or anastomotic. Distant metastasis refers to the presence of metastatic disease at any site other than local regional recurrence. The duration of follow-up was 5 years or until death. The endpoint of this study was PFS. PFS was defined as the time interval from the date of surgery to clinical recurrence or progression.

CT scanning protocol and image preprocessing

258 patients underwent CT scans using Siemens Somatom Definition CT scanner (Munich, Germany). The scanning range was from the thoracic inlet to the diaphragmatic floor, and the patient was supine to complete the scanning with one breath hold. Imaging parameters: 120kVp; 130mAS; rotation time: 0.5s; collimator width: 64 \times 1.25 mm; pitch:1.5:1; field of view: 350 \times 350 mm; matrix:512 \times 512; layer thickness: 5 mm; layer spacing: 5 mm; Following injection of iodinated contrast agent at a rate of 2.5–3.0 ml/s through antecubital vein with high-pressure injector, contrast-enhanced CT scanning was conducted at 25–30 s (arterial phase). A two-step process for image standardization was implemented in this study: (a) image resampling (voxel size of 1 \times 1 \times 1 mm³) and pixel intensity normalizing (the intensity ranges from –1024 to 1024HU and the unified abdomen window (window-level [WL] of 50 and window-width [WW] of 350)

Tumor segmentation and radiomics feature extraction

The software “ITK-SNAP” (www.itksnap.org) was used to process CT images. 2 radiologists with minimum 5 years related experience manually delineated region of interest (ROI) along tumor edge layer after layer to achieve segmentation of lesions. As the heterogeneity of the tumor, the 3D ROI should include the entire lesion, but should avoid the surrounding adipose tissue, blood vessels, lymph nodes, gas and fluid. Image pretreatment and features extraction were performed using an open source Pyradiomics-based software of FAE software (version 0.5.2; <https://github.com/salan668/FAE>)¹⁹. Finally, we extracted 1316 radiomics features from arterial phase-enhanced CT images, including 216 first-order features, 1086 texture features and 14 shape features. The texture features include gray level dependence matrix (GLDM), gray level co-occurrence matrix (GLCM), gray level run length matrix (GLRLM), gray level size zone matrix (GLSZM) and neighboring gray tone difference matrix (NGTDM).

Radiomics feature selection and radiomics signature construction

The best radiomics features were selected through the following four steps. First, Z-score was used to normalize the data. Second, we use cox proportional hazards model with Intra - class correlation coefficients (COX(ICC)) to quantify features reproducibility, which were extracted by two physicians from a randomly selected subset of 30 patients and obtain the radiomics features unaffected by variability in tumor segmentation ($ICC > 0.90$). Third, maximal relevance and minimal redundancy (MRMR) algorithm and F (LASSO) Cox regression were used to perform feature dimension reduction. We used 10-fold cross validation to select the best hyperparameter λ value for penalty parameter tuning in order to identify the top features. Last, we calculated radiomics score (Rad-score) of each patient through linear combination of the selected features and coefficient vector to develop radiomics model.

Inflammatory model construction

We use univariate and multivariate cox regression analysis to select the inflammatory indicators, and the inflammatory model was constructed by using the selected inflammatory indicators.

Radiomics model construction

The best radiomics features were selected by LASSO-Cox regression and 10-fold cross validation. The formula of Rad-score was constructed based on the weighting coefficients corresponding to the chosen radiomics features, and the radiomic model was constructed by Rad-score.

Nomogram model construction and validation

In order to recognize the clinicopathological risk factors related with PFS, we conducted univariate analysis using the Cox proportional hazards model to determine the factors significantly affecting the likelihood of event ($p < 0.05$). We constructed the multivariate Cox proportional hazards model using backward stepwise selection guided by Akaike information criterion (AIC). We calculated hazard ratio (HR) and 95% confidence interval (CI) of each risk factor to evaluate the strength of association between different variables and PFS. A nomogram model was developed to predict 1-year, 3-year, and 5-year PFS. Using Harrell's concordance index (C-index) to assess the accuracy of the nomogram model. Drawing calibration curves to examine the calibration of nomogram model. The selection of radiomics feature and model development were conducted in training set, followed by evaluation in validation set. The workflow of nomogram model was illustrated in Fig. 1.

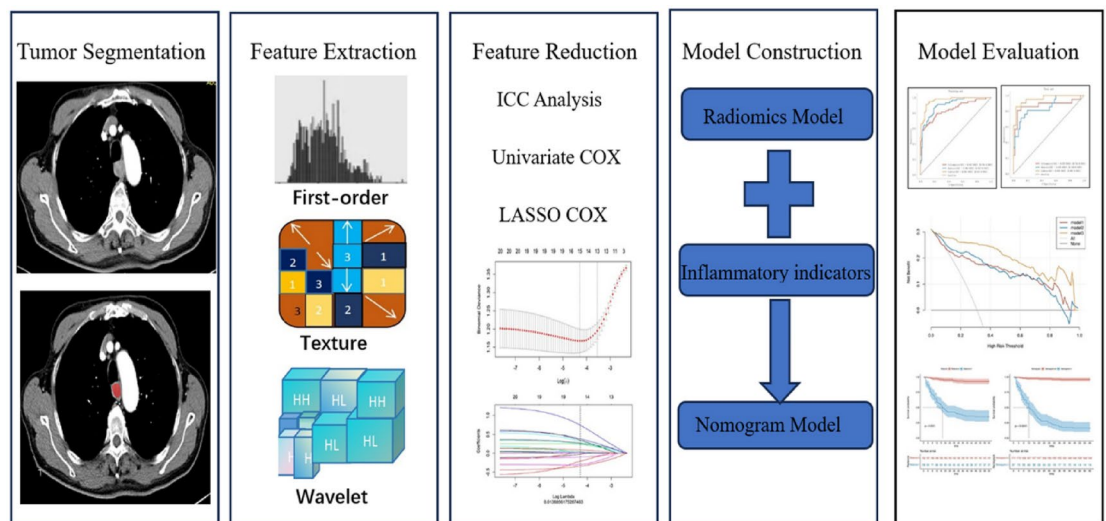


Fig. 1. The workflow of nomogram model. Flow chart illustrating the nomogram model building process. ICC = Intra- and inter-class correlation coefficient; LASSO = Least absolute shrinkage and selection operator.

Statistical analysis

Statistical analysis and graphics production were performed by using R software (Version 4.1.0; <https://www.R-project.org>) and MedCalc (Version 20.100; <https://www.medcalc.org/>). The clinicopathological data were tested for normal distribution by Shapiro Wilk test and for homogeneity of variance by Bartlett test. Continuous variables were represented as means \pm standard deviation, and we compared their distribution by independent t-tests or Wilcoxon rank-sum tests. Categorical variables were compared by chi-square test or Fisher's exact test. We used Cox proportional hazards regression model to evaluate the correlation between relevant clinicopathological factors and PFS. The receiver operating characteristic (ROC) curves were used to analyze the three models, and Delong tests were used to compare the prediction models by area under curve (AUC) values. We also calculated precision-recall curves for each of the three models (inflammatory model, radiomics model, nomogram model) to further evaluate their performance in predicting PFS of ESCC patients. Drawing C-index and calibration curves to assess the nomogram model. C-index was used to evaluate the likelihood that the predicted result was in accordance with actual observation result. As C-index between 0.50 and 0.70 indicates low accuracy, 0.71 to 0.90 indicates moderate accuracy, and higher than 0.90 indicates high accuracy. We divided the patients into high-risk and low-risk group based on the cut-off value of each risk factor in the model, and then survival curves were obtained by using Kaplan-Meier and comparisons were made by using log-rank test. $P < 0.05$ was considered statistically significant.

Results

Clinicopathologic data

The clinicopathological characteristics in this study were summarized in Table 1, and no significant difference was found between the two groups ($P > 0.05$).

Development of inflammatory model

The inflammatory indicators with statistical significance in univariate and multivariate cox regression analysis were as follows (Table 2): (1) LMR (cut-off value ≤ 5.34): the smaller the LMR, the higher the risk of recurrence and progression (HR: 0.741, 95% CI: 0.613–0.896); (2) PLR (cut-off value ≤ 137.97): the smaller the PLR, the higher the risk of recurrence and progression (HR: 0.976, 95% CI: 0.969–0.983); (3) SII (cut-off value > 772.68): the higher the SII, the higher risk of recurrence and progression (HR: 1.002, 95% CI: 1.001–1.003). We included these three variables into inflammatory model to predict PFS of ESCC patients. In training set, inflammatory model had an AUC of 0.847 (95% CI: 0.784–0.908), a sensitivity of 79.7%, and a specificity of 76.9% for predicting PFS of ESCC patients, and an AUC of 0.876 (95% CI: 0.784–0.908) in test set. 0.752–0.978), a sensitivity of 81.0% and a specificity of 94.7%, both with good predictive efficacy.

Development and validation of radiomics model

Firstly, 754 features with ICC > 0.90 revealed high reproducibility in the 1316 features (including 216 first-order features, 1086 texture features and 14 shape features), which were extracted from the ROI of each patient's CT images. Secondly, the MRMR method was used to remove the redundant features and that unrelated with PFS features, remaining 587 features. Lastly, feature selection was performed based on LASSO-Cox regression and 10-fold cross validation, and we used λ as a tuning parameter. Finally, the 15 most relevant features were retained, and then the classification equation was constructed based on the retained features and their corresponding coefficients. The final chosen features and their coefficients were displayed in Fig. 2. The formula of Rad-score was constructed based on the weighting coefficients corresponding to the chosen radiomics features, and the Rad-score of each patient was finally calculated. The radiomics model had the AUC of 0.906 (95% CI: 0.857–0.948), sensitivity of 91.5%, and specificity of 76.0% in training set, and the AUC of 0.855 (95% CI: 0.857–0.948), sensitivity of 81.0% and specificity of 84.7% in test set (95% CI: 0.749–0.949), both with good predictive efficacy.

Development and validation of nomogram model

We combined inflammatory indicators and CT radiomics features to construct a nomogram model (Fig. 3), which included LMR, PLR, SII and Rad-score. The PH hypothesis of the Cox regression model was tested for all variables with P values > 0.05 , indicating that all variables satisfied the equal proportional hazards model. The AUC and C-index of nomogram model in training set were 0.964 (95% CI: 0.938–0.985) and 0.896 (95% CI: 0.867–0.924), respectively. In test set, the values were 0.958 (95% CI: 0.903–0.994) and 0.893 (95% CI: 0.842–0.945), which were better than those of inflammatory model and radiomics model (Table 3; Figs. 4). Significant differences were found between nomogram model and inflammatory model and radiomics model (DeLong test, $Z = 3.869$ and 3.195 , $P < 0.001$, $P = 0.001$). Precision-recall curves for the three models in the training and test set in Fig. 5. In training set (A), the inflammatory and nomogram models show better performance at low recall rates when high precision is prioritized initially. If relatively stable precision during changes in the recall rate is desired, the nomogram model has a greater advantage. In test set (B), for high recall with good precision, the nomogram model is superior. For high precision at low recall, radiomics model performs well in the early stage. While inflammatory model is unstable with large fluctuations. The calibration curve (Fig. 6) indicates good agreement between the prediction and actual observation in training and test set. DCA results of this study (Fig. 7) revealed the net benefit of nomogram model was better than that of inflammatory model and radiomics model within most reasonable probability thresholds, and with the greatest clinical benefit. We used the threshold to classify the Rad-score into high-risk and low-risk group, and Kaplan-Meier analysis was conducted to determine its prognostic value. We calculated the risk threshold to divided nomogram model into low and high-risk group. Kaplan-Meier results demonstrated significant difference of PFS between high-risk

Characteristics	Training set(<i>n</i> = 180)	Test set(<i>n</i> = 78)	<i>P</i> value
Age, median [IQR]	64.50(59.00–71.00)	64.50(59.00–70.00)	0.941
Gender, <i>n</i> (%)			0.388
Female	57(31.67)	29(37.18)	
Male	123(68.33)	49(62.82)	
Neutrophil, median [IQR]	3.99 (3.01–5.24)	4.19 (3.28–5.67)	0.315
Lymphocyte, median [IQR]	1.29(1.04–1.57)	1.30(1.10–1.72)	0.273
Monocyte, median [IQR]	0.36(0.28–0.51)	0.36 (0.29–0.48)	0.859
Platelet, median [IQR]	199.00(152.00–237.25)	229.00(165.00–268.75)	0.056
NLR, median [IQR]	3.04(2.09–4.16)	3.05(2.01–4.91)	0.914
PLR, median [IQR]	148.44(113.52–202.36)	156.39(115.11–215.73)	0.548
LMR, median [IQR]	3.58 (2.56–4.89)	3.54 (2.36–5.27)	0.608
SII, median [IQR]	577.25(409.01–944.02)	649.10(385.45–1037.41)	0.349
Location, <i>n</i> (%)			0.492
Upper	31 (17.22)	9(11.54)	
Middle	90(50.00)	43(55.13)	
Lower	59(32.78)	26(33.33)	
Differentiation, <i>n</i> (%)			0.100
Well	47(26.11)	11(14.10)	
Moderately	102(56.67)	50(64.10)	
Poorly	31(17.22)	17(21.79)	
pT stage, <i>n</i> (%)			0.264
T1	18(10.00)	5(6.41)	
T2	42(23.33)	23(29.49)	
T3	118(65.56)	47(60.26)	
T4	2(1.11)	3(3.85)	
pN stage, <i>n</i> (%)			0.405
N0	80(44.44)	39(50.00)	
N1	65(36.11)	21(26.92)	
N2	23(12.78)	14(17.95)	
N3	12(6.67)	5(6.41)	
LVI, <i>n</i> (%)			0.136
No	95(52.78)	49(62.82)	
Yes	85(47.22)	29(37.18)	
PNI, <i>n</i> (%)			0.765
No	152(84.44)	67(85.90)	
Yes	28(15.56)	11(14.10)	
Radscore, median [IQR]	-0.11[-0.90–0.72]	-0.27[-1.09–0.22]	0.220

Table 1. Clinicopathological characteristics of ESCC patients in training and test set. NLR, neutrophil-to-lymphocyte ratio; LMR, lymphocyte-to-monocyte ratio; PLR, platelet to-lymphocyte ratio; SII, systemic immune inflammation index; LVI, lymphovascular invasion; PNI, perineural invasion.

Inflammatory indicator	Univariate (HR,95%CI)	Cut-off value	<i>P</i> value	Multivariate (HR,95%CI)	<i>P</i> value
NLR	1.082 (1.044–1.123)	> 5.59	< 0.001	0.899 (0.795–1.017)	0.091
LMR	0.752 (0.631–0.896)	≤ 3.4	0.001	0.741 (0.613–0.896)	0.002
PLR	0.990 (0.984–0.995)	> 137.97	< 0.001	0.976 (0.969–0.983)	< 0.001
SII	1.001 (1.000–1.002)	> 772.68	< 0.001	1.002 (1.001–1.003)	< 0.001

Table 2. Results of univariate and multivariate analysis of inflammatory indicator. NLR, neutrophil-to-lymphocyte ratio; LMR, lymphocyte-to-monocyte ratio ; PLR, platelet to-lymphocyte ratio; SII, systemic immune inflammation index; HR, hazard risk; CI, confidence interval.

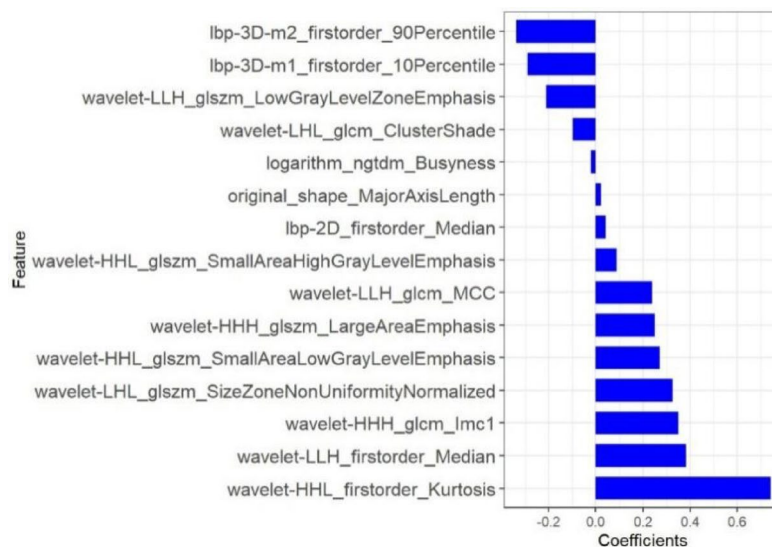


Fig. 2. Weighted graph of radiomics features. Weighted graph of radiomics features show the selected features of radiomics model and its coefficients.

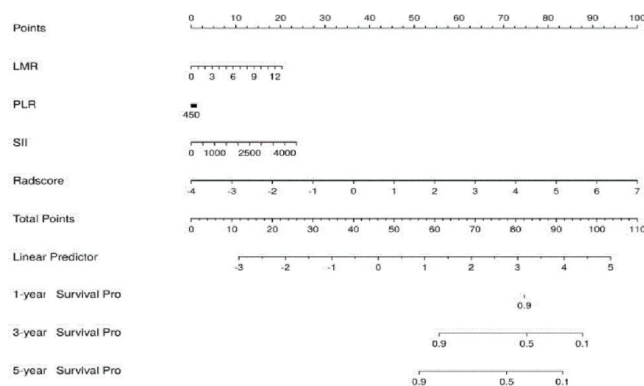


Fig. 3. Nomogram model for predicting PFS in ESCC patient. The nomogram model was developed to predict progression free survival (PFS) in ESCC patient, with LMR, PLR, SII and Rad-score. Points represents the score corresponding to each variable. The total points of each patient were calculated, which represent the prediction of 1-year, 3-year and 5-year survival probability. The prediction probability ranges from 0.1 to 0.9. LMR = lymphocyte-to-monocyte ratio; PLR = neutrophil-to-lymphocyte ratio; SII = systemic immune inflammation index.

Model	Training set		Test set	
	AUC (95%CI)	C-index (95%CI)	AUC (95%CI)	C-index (95%CI)
Inflammatory model	0.847 (0.784–0.908)	0.787 (0.733–0.842)	0.876 (0.752–0.978)	0.813 (0.718–0.908)
Radiomics model	0.906 (0.857–0.948)	0.853 (0.816–0.890)	0.855 (0.749–0.949)	0.804 (0.720–0.888)
Nomogram model	0.964 (0.938–0.985)	0.896 (0.867–0.924)	0.958 (0.903–0.994)	0.893 (0.842–0.945)

Table 3. Comparison of the efficacy of three models in predicting PFS of ESCC. Abbreviations: AUC, area under curve; CI, confidence interval.

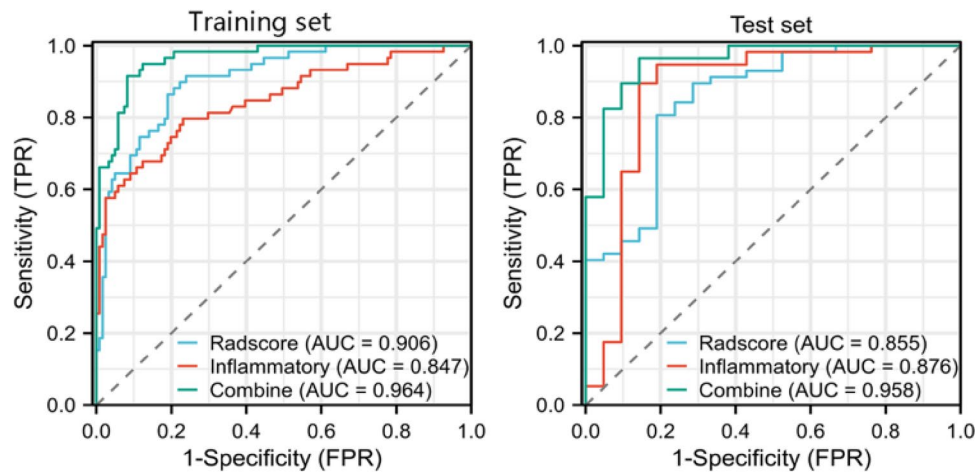


Fig. 4. Comparison of ROC curves of the three models in training set (A) and test set (B). Receiver operating characteristic (ROC) curves reveal that the combined nomogram model has the biggest area under curve (AUC) both in training (A) and test (B) set.

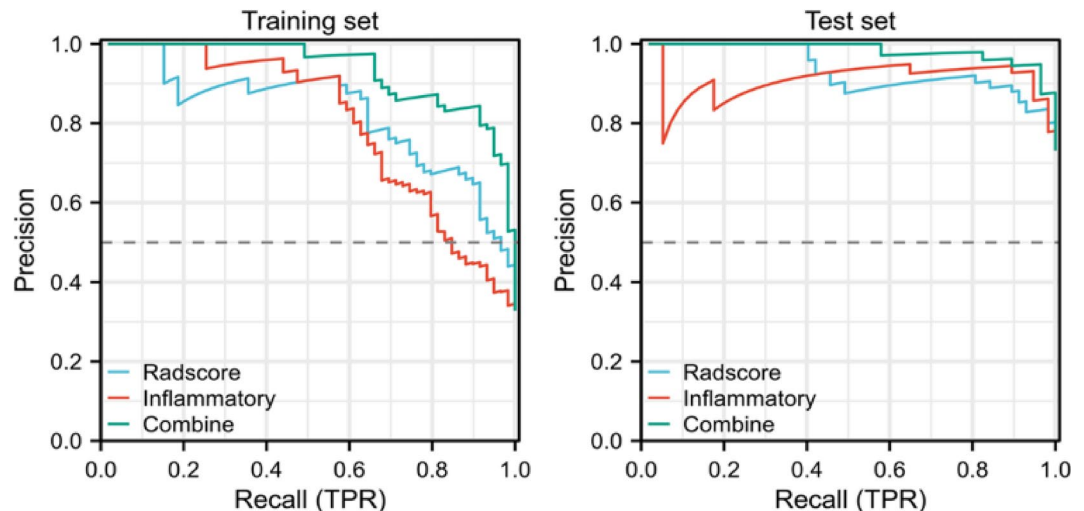


Fig. 5. Precision-recall curves of the three models in training set (A) and test set (B). In the training set (A) and test set (B), the nomogram model shows better overall performance in balancing precision and recall. The radiomics model demonstrates superior precision at low recall rates. The inflammatory model exhibits significant fluctuations and poor stability.

group and low-risk group in radiomics and nomogram model ($P < 0.001$), and high-risk group was prone to postoperative recurrence and with poor PFS (Fig. 8).

Discussion

Radiomics research of esophageal cancer mainly focused on the prediction of lymph node metastasis and the efficacy prediction of radiotherapy and chemotherapy, but there were few studies on the prediction of PFS before surgery. The establishment of an accurate PFS prediction model is beneficial to individualized decision-making and expected to improve the survival rate of ESCC patients. Therefore, we developed and validated a nomogram model of inflammatory indicators combined with radiomics features to predict PFS of ESCC patients after radical resection. C-index and AUC revealed the nomogram model had better performance than radiomics or inflammatory models alone. Our study results confirmed that the predictive efficacy of the nomogram model was enhanced after incorporating inflammatory indicators.

In recent years, numerous studies have validated the practical value of immune-inflammatory indicators in predicting postoperative survival rates in solid tumors. However, the prognostic value for these indicators in esophageal carcinoma patients remain uncertain^{20–22}. Previous studies have shown that low LMR and high PLR are generally associated with poor prognostic factors, such as shorter survival times, increased disease recurrence rates, and higher risks of postoperative complications in ESCC patients^{23,24}. Some studies also

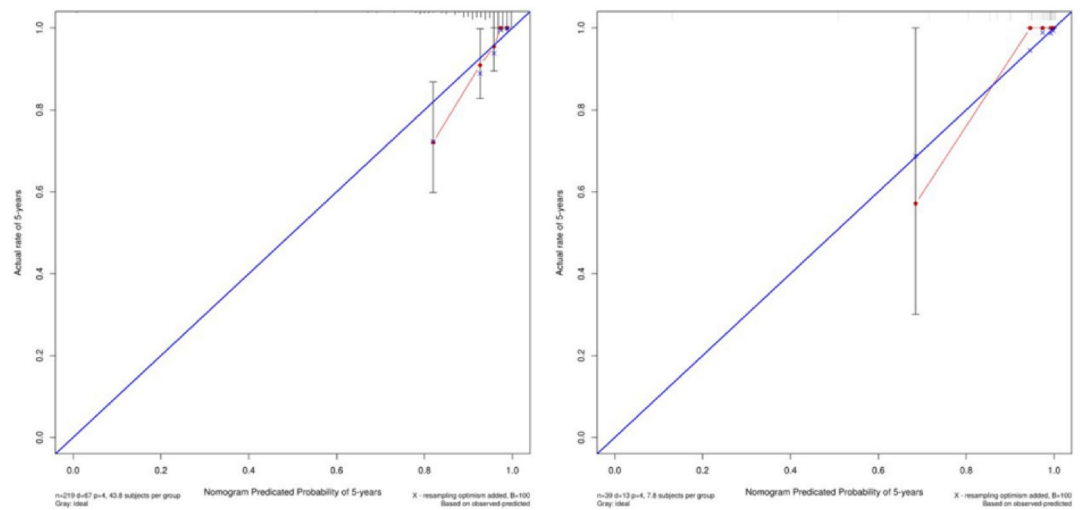


Fig. 6. Calibration curves for training set (A) and test set (B). Calibration curves, with horizontal axis representing the mean predicted probability and vertical axis representing the actual probability of the event. The dark blue line is the reference line, The closer the line is to the reference line, indicating higher accuracy of the model's predictions. The calibration curve in our study indicates good agreement between the prediction and actual observation both in training (A) and test (B) set.

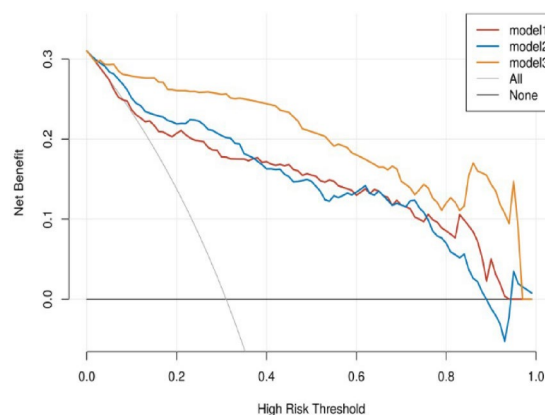


Fig. 7. DCA curve. Decision curve analysis, with horizontal axis representing threshold probability and vertical axis representing net benefit. Black line is on behalf of the patients without recurrence or progress. Gray line is on behalf of the patients with recurrence or progress. Red line is on behalf of inflammatory model. Blue line is on behalf of radiomics model. Orange line is on behalf of nomogram model. And the nomogram model has the highest net benefit.

demonstrated high SII is an independent risk factor for poor prognosis of patients with esophageal carcinoma, and the overall survival time of patients with high SII before treatment is significantly shorter^{25,26}. In our study, Cox regression analysis suggested LMR, PLR, and SII were independent predictive factor for postoperative PFS in ESCC patients, and lower LMR/PLR and higher SII were associated with poor prognosis. Mechanisms by which inflammatory cells affect cancer prognosis: In the tumor microenvironment, inflammatory cells such as neutrophils, lymphocytes, monocytes, and platelets influence tumor progression through a variety of complex mechanisms. Neutrophils can inhibit the immune response, promote cancer cell transformation, and angiogenesis. Lymphocytes can regulate tumor growth, and a decrease in their number will weaken the immune function. Monocytes can differentiate into tumor - associated macrophages, which affects the tumor. Platelets can stimulate tumorigenesis and metastasis. In this study, we incorporated the above three inflammatory variables into the inflammatory model to predict PFS of ESCC patients. In training set, the AUC of inflammatory model for predicting PFS in ESCC patients was 0.847(95%CI: 0.784–0.908), and 0.876 (95%CI: 0.752–0.978) in the test set, with C-index values of 0.787(95%CI: 0.733–0.842) and 0.813(95%CI: 0.718–0.908), indicating good predictive efficiency.

Our study results indicated Rad-score was an independent risk factor for predicting PFS in ESCC patients and could serve as a non-invasive biomarker for risk stratification. We used Rad-score threshold to classify patients into high-risk and low-risk group. Kaplan-Meier analysis revealed that patients with high Rad-score

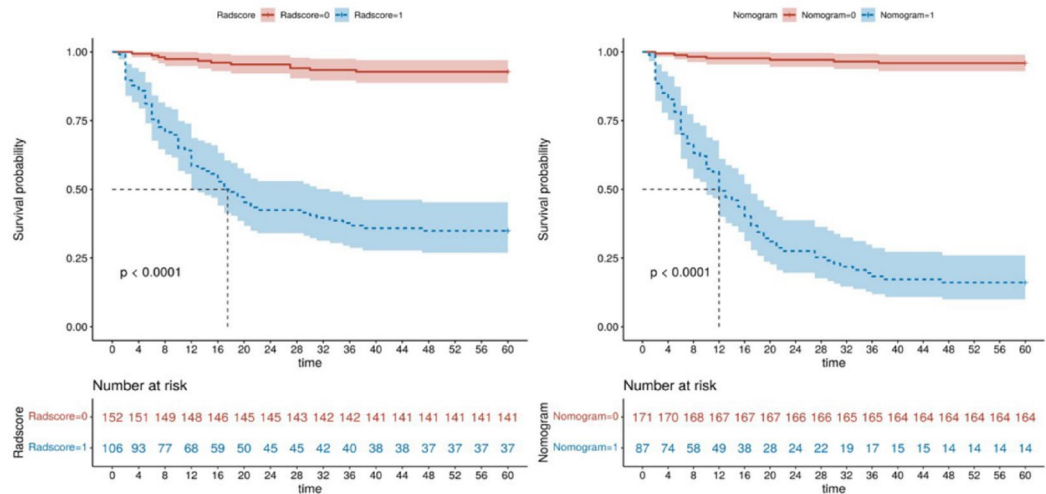


Fig. 8. Kaplan-Meier curves of Radscore (A) and Nomogram (B) in high-risk and low-risk group. Kaplan-Meier analysis of progression free survival (PFS). (A) Kaplan-Meier curves comparing PFS between high-risk Radscore group (blue line) and low-risk Radscore group (red line). (B) Kaplan-Meier curves comparing PFS between high-risk Nomogram group (blue line) and low-risk Nomogram group (red line). As $p < 0.0001$ indicated significant difference of PFS between high-risk group and low-risk group in Rad-score and nomogram model. Besides, as time went on, the high-risk group was prone to with shorter PFS.

had poorer PFS and were more prone to postoperative recurrence and metastasis. The radiomics model contains the information by observing the whole tumor and extracting high-dimensional features such as wavelet and logs, which can provide more information than that from single section, and more prognostic information can be obtained than that collected from clinicopathological factors alone²⁷. Radiomics features can offer a quantitative description of tumor pixel intensity distribution, gray scale distribution as well as variation and frequency range, which can be used to reveal heterogeneity of tumor. In our study, 15 out of 1316 radiomics features could predict PFS in ESCC patients, and wavelet filter provided the most information ($n=10$), indicating that wavelet filter contained more prognostic information. Wavelet features reflect multi-frequency information from multiple dimensions of tumors and offer more effective insight into tumor heterogeneity, which have been applied to a number of radiomics studies²⁸. Previous studies have shown that wavelet features can effectively predict differentiation degree, lymph node metastasis and therapeutic response in ESCC patients, and they have been used to construct radiomics prediction models^{29–31}. These studies indicate wavelet features can be used for prognostic prediction. Our findings are consistent with these results, demonstrating that wavelet features are an important component of radiomics model. One possible explanation for is that multifrequency decomposition of raw CT images provides more comprehensive information of tumor heterogeneity, enabling better prediction of ESCC patients' prognosis. Additionally, first-order radiomics features also showed good predictive performance in our study. Our findings suggested smaller medians and kurtosis were associated with poorer prognosis, and the 10th and 90th percentiles of first-order features with transformed local binary pattern (3D) models were linked to poor prognosis. The 10th and 90th percentiles of tumor intensity features may be associated with micro-vessel density and structure of tumor. Increased angiogenesis, increased density and incomplete structure of esophageal tumors may induce to the increased enhanced degree and malignant degree of tumor, making tumors with obvious heterogeneity¹⁸. Thus, the percentile values of 10th and 90th may reflect intra-tumor heterogeneity, and with higher values indicating greater tumor enhancement and worse prognosis, consistent with findings from Choe et al.³² in lung adenocarcinoma patients.

In this study, we constructed a combined nomogram model by integrating Rad-score and inflammatory indicators to predict PFS in ESCC patients. There are multiple correlations between tumor radiomics features and inflammatory indicators, and this correlation is of great significance for the diagnosis, treatment, and prognosis assessment of tumor. Firstly, the growth and development of tumor rely on the inflammatory microenvironment, in which inflammatory cells, cytokines, chemokines, etc. play important roles. Some radiomics features may be related to the degree of infiltration of inflammatory cells within the tumor. Secondly, tumor angiogenesis is a crucial link in tumor growth and metastasis and is also closely related to inflammation. In radiomics, the blood vessel - related features of tumor are correlated with inflammatory indicators. An increase in serum inflammatory indicators may indicate an enhanced inflammatory response, which is also associated with increased tumor angiogenesis, thus affecting the imaging manifestations of the tumor. Besides, inflammation plays an important role in the invasion and metastasis of tumor. Inflammation - related factors can promote the migration and invasion of tumor cells. An increase in inflammatory indicators may also be associated with the risk of distant metastasis of tumor, and radiomics features can be used to assess the possibility of tumor metastasis. The combined analysis of tumor radiomics features and inflammatory indicators can more accurately predict the prognosis of patients. In our study, the AUC and C-index of nomogram model for predicting PFS in training set were 0.964 (95%CI: 0.938–0.985) and 0.896 (95%CI: 0.867–0.924), respectively. In test set, the values

were 0.958 (95%CI:0.903–0.994) and 0.893 (95%CI: 0.842–0.945), which were better than those of inflammatory model and radiomics model. In addition, the DCA results of this study suggested nomogram model was better than inflammatory model and radiomics model in most reasonable probability thresholds, and had the greatest clinical benefit. Kaplan-Meier curve analysis showed the high-risk group in nomogram model had significantly shorter PFS and higher recurrence and progression rate. Qiu et al.³ and Tang et al.⁶ used radiomics and clinical features to build a nomogram model to predict the prognostic value of ESCC patients treated with neoadjuvant therapy, which were similar to our study, the difference were that our nomogram model includes multiple inflammatory indicators, which could provide more reference information for clinical practice, so as to provide more valuable information for personalized treatment and monitoring of tumor.

Nomogram model in our study shows good accuracy in predicting 5-year PFS in ESCC patients after surgery. However, some limitations exist in this study. Firstly, esophageal peristalsis can lead to variations in radiomics features, the accuracy and stability of manual tumor delineation may affect the standardization and repeatability of the results. Secondly, our study lacks external validation. Although we used DCA to evaluate the clinical efficacy of the combined nomogram model, future multicenter studies are needed to assess the generalization ability of our findings. Lastly, genomic features were not included in our study. Tumor genetic phenotype may explain interindividual differences in survival prognosis at the biological level, and their inclusion could further enhance the predictive power of the model.

Conclusion

This study proposes a novel non-invasive prognostic indicator based on contrast-enhanced CT radiomics features, which can improve prognostic prediction ability for ESCC. The nomogram model developed by combining inflammatory indicators and radiomics features successfully divided patients into high-risk and low-risk group, which is helpful for risk stratification, tumor monitoring and follow-up work, provides important value for precise treatment of ESCC patients, and provides an opportunity for clinicians to formulate personalized strategies to improve patient prognosis.

Data availability

The datasets presented in this article are owned by the affiliated Huaian No.1 People's Hospital of Nanjing Medical University and are not made public. Requests to access these datasets should be directed to corresponding author WC, wchen74@163.com.

Received: 29 November 2024; Accepted: 5 May 2025

Published online: 10 May 2025

References

1. Ajani, J. A. et al. Esophageal and esophagogastric junction cancers, version 2.2019, NCCN clinical practice guidelines in oncology. *J. Natl. Compr. Canc Netw.* **17**, 855–883 (2019).
2. Kakeji, Y. et al. Multimodality approaches to control esophageal cancer: Development of chemoradiotherapy, chemotherapy, and immunotherapy. *Esophagus* **18**, 25–32 (2021).
3. Qiu, Q. et al. Development and validation of a radiomics nomogram model for predicting postoperative recurrence in patients with esophageal squamous cell cancer who achieved pCR after neoadjuvant chemoradiotherapy followed by surgery. *Front. Oncol.* **10**, 1398 (2020).
4. He, Y. et al. Clinical characteristics and survival of 5283 esophageal cancer patients: A multicenter study from eighteen hospitals across six regions in China. *Cancer Commun. (Lond.)* **40**, 531–544 (2020).
5. Zhang, W. Y., Chen, X. X., Chen, W. H., Zhang, H. & Zou, C. L. Nomograms for predicting risk of locoregional recurrence and distant metastases for esophageal cancer patients after radical esophagectomy. *BMC Cancer* **18**, 879 (2018).
6. Tang, S. et al. Application of contrast-enhanced CT radiomics in prediction of early recurrence of locally advanced esophageal squamous cell carcinoma after trimodal therapy. *Cancer Imaging* **21**, 38 (2021).
7. Xie, H. et al. The inflammatory burden index is a superior systemic inflammation biomarker for the prognosis of non-small cell lung cancer. *J. Cachexia Sarcopenia Muscle* **14**, 869–878 (2023).
8. Yin, C. et al. Clinical significance of the preoperative inflammatory burden index in esophageal cancer. *Oncol. D Oi.* <https://doi.org/10.1159/000535727> (2023).
9. Xie, H. L. et al. Inflammatory burden as a prognostic biomarker for cancer. *Clin. Nutr.* **41**, 1236–1243 (2022).
10. Hirahara, N. et al. A novel prognostic scoring system using inflammatory response biomarkers for esophageal squamous cell carcinoma. *World J. Surg.* **42**, 172–184 (2018).
11. Sun, Y. W., Huang, Z. K. & Chi, P. An inflammation index-based prediction of treatment response to neoadjuvant chemoradiotherapy for rectal mucinous adenocarcinoma. *Int. J. Clin. Oncol.* **25**, 1299–1307 (2020).
12. Vernuccio, F. et al. Radiomics and artificial intelligence: New frontiers in medicine. *Recent. Prog. Med.* **111**, 130–135 (2020).
13. O'Connor, J. P. et al. Imaging biomarker roadmap for cancer studies. *Nat. Rev. Clin. Oncol.* **14**, 169–186 (2017).
14. Zhao, B. et al. CT radiomics in the identification of preoperative under staging in patients with clinical stage T1–2N0 esophageal squamous cell carcinoma. *Quant. Imaging Med. Surg.* **13**, 7996–8008 (2023).
15. Gong, J. et al. CT-based radiomics nomogram May predict local recurrence-free survival in esophageal cancer patients receiving definitive chemoradiation or radiotherapy: A multicenter study. *Radiother Oncol.* **174**, 8–15 (2022).
16. Wu, L. et al. Radiomics approach for preoperative identification of stages I–II and III–IV of esophageal cancer. *Chin. J. Cancer Res.* **30**, 396–405 (2018).
17. Yang, Y. et al. A combined nomogram based on radiomics and hematology to predict the pathological complete response of neoadjuvant immunochemotherapy in esophageal squamous cell carcinoma. *BMC Cancer* **24**, 460 (2024).
18. Geng, X. et al. Radiomics-clinical nomogram for preoperative lymph node metastasis prediction in esophageal carcinoma. *Br. J. Radiol.* **97**, 652–659 (2024).
19. Song, Y. et al. FeAture explorer (FAE): A tool for developing and comparing radiomics models. *PLoS One* **15**, e0237587 (2020).
20. Aoyama, T. et al. The prognostic immune and nutritional indices are independent prognostic factors for esophageal Cancer patients who receive curative treatment. *Anticancer Res.* **44**, 2185–2192 (2024).
21. Aoyama, T. et al. Lymphocyte to monocyte ratio is an independent prognostic factor in patients with esophageal cancer who receive curative treatment. *Anticancer Res.* **44**, 339–346 (2024).

22. Hirahara Noriyuki, M. et al. Prognostic value of preoperative inflammatory response biomarkers in patients with esophageal cancer who undergo a curative thoroscopic esophagectomy. *BMC Surg.* **16**, 66 (2016).
23. Xu, X. Q. & Jing, J. X. Inflammation-related parameter serve as prognostic biomarker in esophageal squamous cell carcinoma. *Front. Oncol.* **12**, 900305 (2022).
24. Sun, Y. G. & Zhang, L. F. The clinical use of pretreatment NLR, PLR, and LMR in patients with esophageal squamous cell carcinoma: Evidence from a meta-analysis. *Cancer Manag. Res.* **10**, 6167–6179 (2018).
25. Obata Yuma, K. et al. The preoperative systemic immune-inflammation index is associated with an unfavorable prognosis for patients undergoing curative resection of esophageal squamous cell carcinoma after neoadjuvant therapy. *Surg. Today.* **53**, 964–972 (2023).
26. Zeng, X. X. et al. Prognostic value of pretreatment systemic immune-inflammation index in Chinese esophageal squamous cell carcinoma patients receiving radical radiotherapy: A meta-analysis. *Med. (Baltim).* **102**, e34117 (2023).
27. Cai, C. et al. Multiparametric MRI-based radiomics signature for preoperative Estimation of tumor-stroma ratio in rectal cancer. *Eur. Radiol.* **31**, 3326–3335 (2021).
28. Soufi, M., Arimura, H. & Nagami, N. Identification of optimal mother wavelets in survival prediction of lung cancer patients using wavelet decomposition-based radiomic features. *Med. Phys.* **45**, 5116–5128 (2018).
29. Kawahara, D., Murakami, Y., Tani, S. & Nagata, Y. A prediction model for degree of differentiation for resectable locally advanced esophageal squamous cell carcinoma based on CT images using radiomics and machine-learning. *Br. J. Radiol.* **94**, 20210525 (2021).
30. Tan, X. et al. Radiomics nomogram outperforms size criteria in discriminating lymph node metastasis in resectable esophageal squamous cell carcinoma. *Eur. Radiol.* **29**, 392–400 (2019).
31. Luo, H. S. et al. A nomogram based on pretreatment CT radiomics features for predicting complete response to chemoradiotherapy in patients with esophageal squamous cell cancer. *Radiat. Oncol.* **15**, 249 (2020).
32. Choe, J. et al. Outcome prediction in resectable lung adenocarcinoma patients. Value of CT radiomics. *Eur. Radiol.* **30**, 4952–4963 (2020).

Author contributions

Yating Wang: Writing – original draft; investigation; methodology; writing – review and editing. Genji Bai: Supervision; project administration; writing – review and editing. Min Huang: Formal analysis; visualization; Wei Chen: Conceptualization; resources; software; data curation; formal analysis; validation; writing – review and editing.

Declarations

Competing interests

The authors declare no competing interests.

Ethics statement

The studies involving human participants were reviewed and approved by Institutional review board of the Affiliated Huaian No.1 People's Hospital of Nanjing Medical University (KY-2022-045-01). Written informed consent for participation was not required for this study in accordance with the national legislation and the institutional requirements.

Additional information

Supplementary Information The online version contains supplementary material available at <https://doi.org/10.1038/s41598-025-01240-7>.

Correspondence and requests for materials should be addressed to W.C.

Reprints and permissions information is available at www.nature.com/reprints.

Publisher's note Springer Nature remains neutral with regard to jurisdictional claims in published maps and institutional affiliations.

Open Access This article is licensed under a Creative Commons Attribution-NonCommercial-NoDerivatives 4.0 International License, which permits any non-commercial use, sharing, distribution and reproduction in any medium or format, as long as you give appropriate credit to the original author(s) and the source, provide a link to the Creative Commons licence, and indicate if you modified the licensed material. You do not have permission under this licence to share adapted material derived from this article or parts of it. The images or other third party material in this article are included in the article's Creative Commons licence, unless indicated otherwise in a credit line to the material. If material is not included in the article's Creative Commons licence and your intended use is not permitted by statutory regulation or exceeds the permitted use, you will need to obtain permission directly from the copyright holder. To view a copy of this licence, visit <http://creativecommons.org/licenses/by-nc-nd/4.0/>.

© The Author(s) 2025